Front. Struct. Civ. Eng. 2012, 6(1): 44–52
DOI 10.1007/s11709-012-0138-x

RESEARCH ARTICLE

Efficiency of scalar and vector intensity measures for seismic slope displacements

Gang WANG

Department of Civil and Environmental Engineering, Hong Kong University of Science and Technology, Hong Kong, China
**Corresponding author. E-mail: gwang@ust.hk*

ABSTRACT Ground motion intensity measures are usually used to predict the earthquake-induced displacements in earth dams, soil slopes and soil structures. In this study, the efficiency of various single ground motion intensity measures (scalar *IMs*) or a combination of them (vector *IMs*) are investigated using the PEER-NGA strong motion database and an equivalent-linear sliding-mass model. Although no single intensity measure is efficient enough for all slope conditions, the spectral acceleration at 1.5 times of the initial slope period and Arias intensity of the input motion are found to be the most efficient scalar *IMs* for flexible slopes and stiff slopes respectively.

Vector *IMs* can incorporate different characteristics of the ground motion and thus significantly improve the efficiency over a wide range of slope conditions. Among various vector *IMs* considered, the spectral accelerations at multiple spectral periods achieve high efficiency for a wide range of slope conditions. This study provides useful guidance to the development of more efficient empirical prediction models as well as the ground motion selection criteria for time domain analysis of seismic slope displacements.

KEYWORDS seismic slope displacements, intensity measures, empirical prediction

1 Introduction

Realistic prediction of the permanent displacements in earth dams, soil slopes and soil structures under earthquake loading is an important topic for evaluating and mitigating seismic hazards. Since Newmark's pioneering work on the rigid sliding block method [1], extensive research has been focused on finding the suitable ground motion parameters that can be reliably used to estimate the earthquake-induced displacements in earth dams, earth embankments and slopes. As earthquake records are complex transient time series, different ground motion intensity measures (*IMs*) can only represent certain aspects of ground motion characteristics. Some single intensity measures (termed scalar *IMs*), such as the peak ground acceleration (*PGA*), were often used in the Newmark-type rigid sliding block models [2–4]. Other scalar *IMs* such as the dominant period of the earthquake motion and Arias Intensity (*IA*) have also been used [3,5,6]. Using multiple intensity measures (termed vector *IMs*) has also been considered, for example in Ref. [7]. It should be noted that all of the above research assume that the slope behaves as a rigid-plastic material, and slope displacement is calculated by double integrating the part of the input acceleration that exceeds a critical value. The Newmark-type rigid sliding block model provides a simple index of dynamic slope performance. However, it is only appropriate for shallow landslides of stiff materials (e.g., rock blocks) that move along a well-defined slip surface.

To better understand the influence of soil nonlinearity on seismic slope response, Bray and his coworkers [8,9] have conducted numerical simulations using a simple nonlinear stick-slip model. In this model, the soil slope is simplified as a generalized single-degree-of-freedom system governed by the first modal shape of vibration. Nonlinear properties of soils are modeled using an equivalent-linear method, similar to the well-known SHAKE analysis [10], such that the stiffness and damping ratio of the system is modified to be compatible with the induced strain level during shaking. Irreversible permanent displacements would occur if the base acceleration exceeds a prescribed critical value. In this model, the dynamic characteristic is characterized by the initial (small-strain) period of the

Article history: Received December 5, 2011; Accepted December 29, 2011

slope (T_s) and the strength of the earth slope is represented by the yield acceleration (K_y). Soil nonlinearity causes elongation of the slope period during shaking, and the most efficient scalar *IM* for the earthquake-induced displacements has been found to be the spectral acceleration at 1.5 times the initial period of the system. The standard deviation of the model is 0.67 (in natural log units) for all slope conditions [9].

The previous study focused on using a scalar *IM* to develop empirical predictive models for seismic slope displacements. Large uncertainties in existing methods demonstrate that no scalar *IM* can accurately predict slope displacement. Using vector *IMs* allows for a better representation of different aspects of ground motions and thus significantly improves the accuracy of slope displacement prediction. Yet, the efficiency of scalar and vector *IMs* has not yet been fully investigated. This study will systematically evaluate the efficiency of various scalar *IMs* and vector *IMs* in correlating with the seismic slope displacements considering different slope conditions. The results provide insight to improve the efficiency of empirical models as well as the ground motion selection methods for time domain analysis of seismic slope displacements.

2 Ground motion intensity measures

Earthquake acceleration time histories are chosen from the PEER-NGA strong motion database [11] (http://peer.berkeley.edu/nga/). The database contains a total of 173 earthquakes from California, Japan, Taiwan and other seismic active regions, with a total of 3551 three-directional acceleration time histories. Only horizontal recordings from free-field conditions are used in the analysis, resulting in a total of 1560 pairs of ground motions of two horizontal directions. The equivalent-linear sliding mass model [8,9] is used in the present study. The detailed mathematical formulation of the model is summarized in Appendix. The permanent displacements of the sliding mass were computed using each of the as-recorded earthquake motions in the database. Two orthogonal recordings at the same station are treated as separate records. For each record, the permanent displacements were calculated by applying the record in the positive and the negative directions, and the maximum value of two directions was taken as the permanent displacement for that record. Figure 1(a) shows the computed permanent displacement using acceleration time history recorded during Superstition Hills Earthquake (1987) at USGS Station 286. The yield acceleration K_y is assumed to be 0.1 g and the site period T_s varies from 0 to 2 s. If the slope is rigid (T_s = 0 s), the permanent sliding displacement is 46 cm. The permanent displacement reaches approximately 90 cm if the site period falls into the range of 0.1–0.4 s due to the resonance of the site with the concentrated shaking energy at that period range (note the mean period of the record 0.38 s). As the slope becomes more flexible (T_s increases), the permanent displacement decrease to a negligible value if the site period is greater than 1 s. We assumed that the shear wave velocity of the soil is 250 m/s. During the shaking, the modulus reduction and damping ratio curves follow that for clays with plasticity index of 30 [12], as is illustrated in Fig. 1(b).

In this study, we consider several most commonly used intensity measures to characterize the ground motion time histories. The definitions of these *IMs* are summarized in Table 1. One may also refer to standard reference books for detailed explanation, e.g., Ref. [13]. The scalar *IMs* considered can be roughly categorized into the following groups: 1) *IMs* that are related to the peak amplitude of the

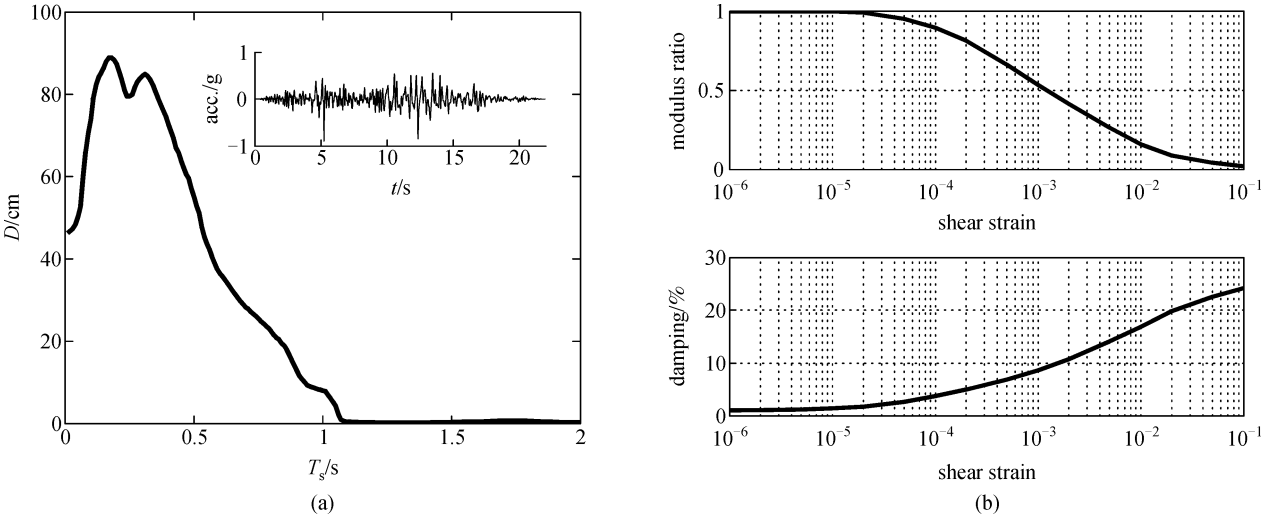

Fig. 1 (a) Computed permanent displacements (K_y = 0.1 g). Insert: acceleration time history; (b) modulus ratio and damping curve for nonlinear soils

Table 1 Definition of scalar *IMs*

IM	name	definition	units
PGA	peak ground acceleration	$\max_t \lvert a(t)\rvert$, the maximum absolute value of the acceleration time history	g
Sa	spectral acceleration	Sa(T), peak acceleration of a single-DOF elastic oscillator with specified period T and 5% damping ratio	g
ASI	acceleration spectrum intensity	$\int_{T=0.1}^{0.5s} Sa(T)\mathrm{d}T$, integration of Sa($T$) over T = 0.1 s to 0.5 s.	g
IA	Arias intensity [14]	$\frac{\pi}{2g}\int_0^\infty \lvert a(t)\rvert^2\mathrm{d}t$, time integration of the acceleration squared	g·s
CAV	cumulative absolute velocity	$\int_0^\infty \lvert a(t)\rvert\mathrm{d}t$, time integration of the absolute value of acceleration.	g·s
$D_{5\text{-}95}$	significant duration [15]	$t(0.95IA)$-$t(0.05IA)$, time used to accumulate from 5% to 95% *IA*	s
T_m	mean period [16]	weighted mean period of Fourier spectrum	s

ground motion time history, i.e., the peak ground acceleration (*PGA*); 2) *IMs* that are related to the frequency content of the ground motion, i.e., the spectral acceleration at initial site period, $Sa(T_s)$, and the spectral acceleration at 1.5 times of initial site period, $Sa(1.5T_s)$; 3) the integration of the spectral acceleration over a range of spectral periods such as acceleration spectrum intensity (*ASI*). 4) The time integration of the acceleration time history, representing certain kind of seismic energy, i.e., Arias intensity (*IA*) [14] and cumulative acceleration velocity (*CAV*); (5) the duration of the ground motion, i.e., the significant duration ($D_{5\text{-}95}$) [15], and 6) the mean period of the earthquake motion (T_m) [16]. These *IMs* represents different aspects of the ground motion characteristics and are commonly used in earthquake engineering design.

For each ground motion in the strong motion database, the seismic slope displacement can be computed. Figures 2 and 3 present the scatter plots of computed seismic slope displacements against the scalar *IMs* of each ground motion record. The slope resistance is assumed to be K_y = 0.1 g in this example. From these plots, it is evident that some *IMs* are better correlated with the displacements than the others. It may be desirable to use the best correlated *IMs* to develop empirical models such that increased accuracy and reduced uncertainty can be achieved. However, the predictive capacity of an *IM* changes with the properties of the slopes when comparing Fig. 2 (T_s = 0.1 s) with Fig. 3 (T_s = 1 s). In these cases, an *IM* that is closely correlated to the seismic displacements of stiff slopes (e.g., T_s = 0.1 s) may not be a good predictor for flexible slopes (e.g., T_s = 1 s). The objective of the present study is to evaluate the efficiency of these scalar *IMs* and their vector combinations under different slope conditions. Although it is out of the scope of this study, the results can provide significant insights to identify suitable *IMs* for use in empirical prediction models.

3 Efficiency of scalar intensity measures

Using 1560 pairs of ground motion records from the strong motion database and the idealized sliding mass model, earthquake-induced displacements are calculated for various slope conditions. The initial slope period, T_s, ranges from 0.01 s to 2 s. It should be noted that the initial periods of slopes usually fall between 0.2 s and 0.7 s, so there is little practical importance to consider slope periods greater than 2 s. Different levels of yield acceleration K_y is specified from 0.01 g to 0.5 g. For each (T_s, K_y) case, regression analysis was performed by assuming that the seismic displacements D (in natural log unit) are related to the scalar or vector *IMs* (in natural log unit) in the following quadratic form:

$$\ln D = a + \sum_{i=1}^{n} b_i \ln IM_i + \sum_{i=1}^{n} c_i (\ln IM_i)^2 + \varepsilon \cdot \sigma_{\ln D}, \quad (1)$$

where IM_i (i = 1,2,…,n) represents a particulars scalar *IM* that may be combined to form vector *IMs*, and n is the total number of *IMs* used (note n = 1 for the special case when a scalar *IM* is used). Parameters a, b_i, c_i are fitting parameters to be determined for given T_s and K_y. The standard deviation of residuals is $\sigma_{\ln D}$, and ε is a random variable following standard normal distribution. To evaluate the efficiency of *IMs*, the adjusted coefficients of determination (R^2_{adj}) is used. The R^2_{adj} adjusts for the number of regressors through modification of coefficients of determination R^2,

$$R^2_{adj} = 1 - (1 - R^2)\frac{N-1}{N-p-1}, \quad (2)$$

$$R^2 = 1 - \frac{\sum_{k=1}^{N}\left(\ln \hat{D}^{(k)} - \ln D^{(k)}\right)^2}{\sum_{k=1}^{N}\left(\ln \hat{D}^{(k)} - \frac{1}{N}\sum_{i=1}^{N}\ln \hat{D}^{(k)}\right)^2}, \quad (3)$$

where p is the total number of regressors (p = 2n, not counting the constant term), N is the sample size. $\ln \hat{D}^{(k)}$ and $\ln D^{(k)}$ are the-k^{th} observed and predicted values. R^2 is the ratio of explained variation to the total variation of the

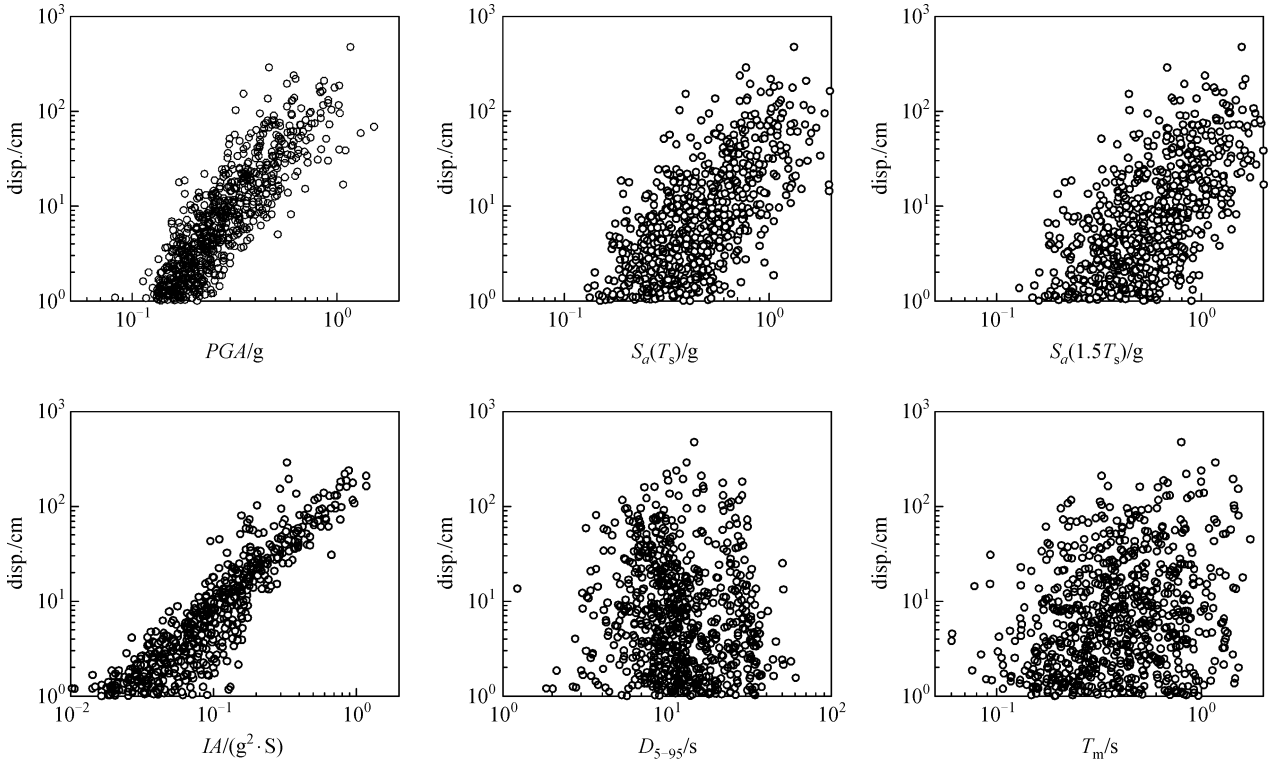

Fig. 2 Seismic displacements vs. *IMs* for a stiff slope (K_y = 0.1 g, T_s = 0.1 s)

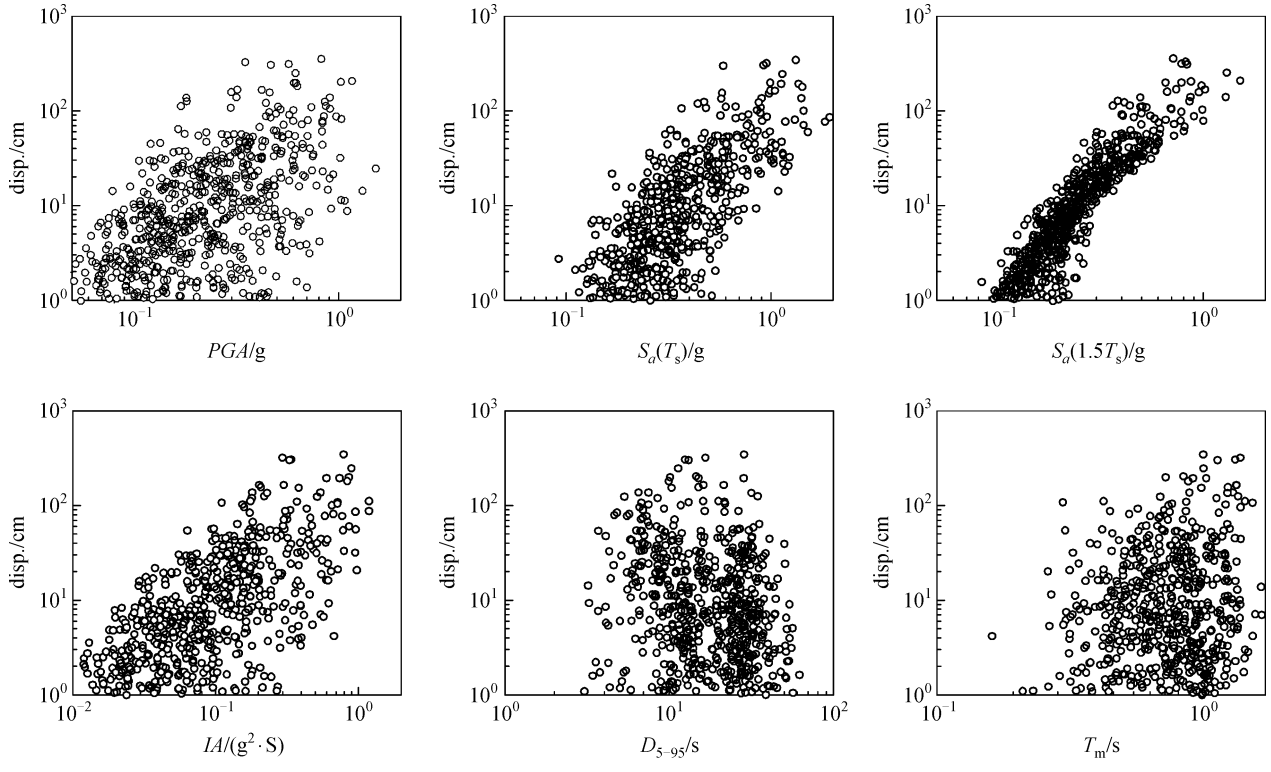

Fig. 3 Seismic displacements vs. *IMs* for a flexible slope (K_y = 0.1 g, T_s = 1 s)

data, and it measures the predictive power of the empirical regression. R^2 ranges from 0 (no predictive power) to 1 (completely predictive). Correspondingly, the maximum value of R^2_{adj} is 1, and it can become a negative number. The value of R^2_{adj} is a good indicator for the efficiency of *IMs*, and it increases only if new term improves the model more than that would be expected by chance. In general, a larger value of R^2_{adj} implies a smaller standard deviation of residuals, thus more efficient in empirical prediction.

Using selected scalar *IMs* as predictors, contours of R^2_{adj} values were computed for slopes of different T_s and K_y are shown in Fig. 4. It is worth mentioning that the analysis is based only on seismic displacements that are greater than 1 cm. Displacements smaller than 1 cm usually causes little engineering consequence. However, the scatter of these data in log space is much larger than the others. Therefore, data elimination is necessary to avoid empirical correlation being controlled by these small-valued data. Furthermore, R^2_{adj} will not be calculated if the number of data are less than 30 in order to guarantee that the sample size is big enough for statistical analysis. The efficiency of each scalar *IM* is summarized as follows:

By definition, the spectral acceleration at the initial site period, $Sa(T_s)$, represents the peak acceleration of a single-degree-of-freedom visco-elastic oscillator of period T_s subjected to the earthquake shaking. Due to nonlinearity of the sliding mass system, $Sa(T_s)$ is no longer an effective intensity measure, as shown in Fig. 4(a), R^2_{adj}<6 for most cases. Instead, elongation of the slope vibration period makes the spectral acceleration at an elongated period a better *IM*. In an earlier study [9], $Sa(1.5T_s)$ was proposed as the most efficient scalar *IM*. As shown in Fig. 4(b), using $Sa(1.5T_s)$ can indeed significantly improve the prediction ($R^2_{adj} > 0.7$) especially for slopes with site periods longer than 0.2 s. However, the efficiency of $Sa(1.5T_s)$ greatly decreases (R^2_{adj}<0.5) if the slope becomes stiffer ($T_s < 0.2$ s), where the efficiency is only slightly higher than that of $Sa(T_s)$.

Compared with the spectral acceleration, *PGA* has much improved efficiency for stiff slope cases ($T_s < 0.2$ s). It is most efficient when T_s is within 0.1 s to 0.3 s, and the efficiency decreases when T_s increases. Similar behavior can be observed from *ASI*, which is the integrated spectral acceleration over the spectral periods from 0.1 s to 0.5 s. The efficiency of *ASI* only slightly decreases with increasing K_y when T_s is within 0.1 s to 0.3 s.

It is interesting to compare the efficiency of *IA* and *CAV* side by side. *IA* is derived from time integration of the square of the entire acceleration time history, and *CAV* is

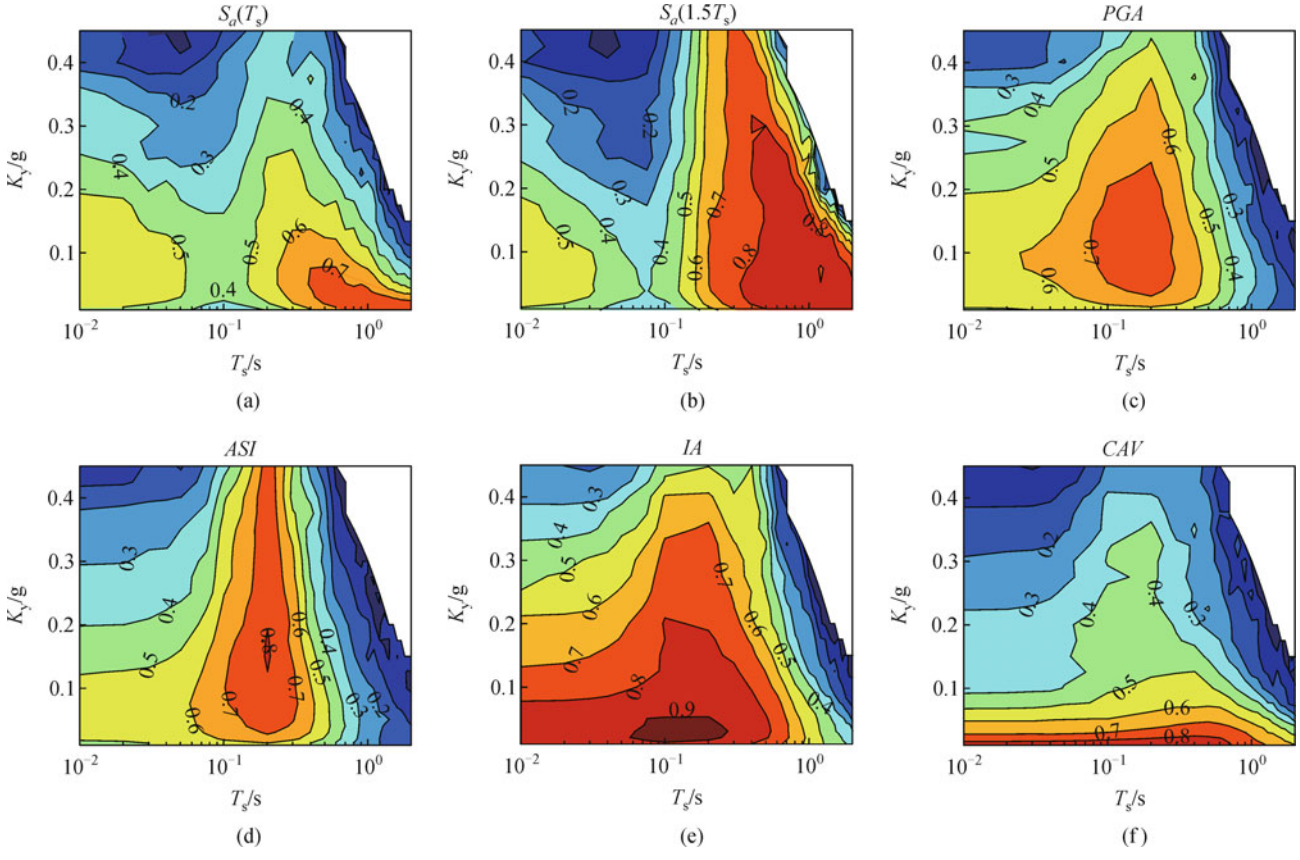

Fig. 4 Contours of adjusted coefficients of determination for scalar *IMs*

time integration of the absolute value of acceleration time history. Both of them implicitly consider the amplitude and the duration of the ground motion. However, as shown in Figs. 4(e) and (f), the overall efficiency of *IA* is much better than that of *CAV* since high efficiency is achieved for a wider range of slope conditions. *CAV* is only marginally better than *IA* in the cases of very small K_y and long slope period T_s. Among all scalar *IMs* that have been considered so far, *IA* is the most efficient *IM* for stiff slope cases.

Similarity in the efficiency of *PGA* and *IA* can be attributed to their strong correlation (correlation coefficient between *IA* and *PGA* is 0.8). However, we also emphasize the improved efficiency of *IA* for the cases of a stiff sliding mass with weak sliding resistance (i.e., $T_s < 0.1$ s and $K_y < 0.2$ g). Under these conditions, the cumulative quantity of the entire time history correlates with the sliding displacement more effectively than an instantaneous spike in the time sequence. One might attribute the improvement of *IA* to its implicit consideration of duration in the formulation. However, further investigation reveals that the significant duration, $D_{5\text{-}95}$, has virtually no correlation with the seismic displacements for all slope conditions ($R^2_{adj} < 0.1$ for most cases, refer to Figs. 2 and 3 for two special cases). Similarly, the mean period T_m of the ground motion has almost no predictive power at all.

The above analysis shows that the efficiency of scalar *IMs* varies with slope conditions, and there is no single scalar *IM* that is efficient to predict seismic displacements for all slope conditions. The finding is consistent with a previous study conducted for some special cases [17]. Using vector *IMs* allows for different characteristics of the ground motions to be considered collectively. Therefore, it is expected that the overall predictive efficiency can be improved.

4 Efficiency of vector intensity measures

Since $Sa(1.5T_s)$ and *IA* are the most efficient scalar *IMs* for flexible slope cases ($T_s > 0.2$ s) and stiff slope cases ($T_s < 0.2$ s) respectively, the vector *IM* that incorporates both of them (termed as "$Sa(1.5T_s) + IA$") can improve the overall efficiency for all slope conditions. As is shown in Fig. 5 (a), $R^2_{adj} > 0.8$ is achieved for slope conditions with $K_y < 0.1$ g and $T_s < 2$ s. The "$Sa(1.5T_s) + IA$" scheme has obvious advantage comparing with "$Sa(1.5T_s) + CAV$" and "$Sa(1.5T_s) + PGA$" combinations. It should be noted that Bray and Travasarou [9] recommended using $Sa(1.5T_s)$ for $T_s > 0.05$ s and *PGA* for $T_s < 0.05$ s in their empirical model. However, their approach is obviously less efficient than using the "$Sa(1.5T_s) + IA$" scheme.

One limitation of using $Sa(1.5T_s)$ as a predictor is that one has to have the prior knowledge of the slope period. For some cases, it is difficult to estimate the slope period accurately. The situation could result in increased uncertainty in seismic displacement prediction using these property-dependent *IMs*. It is therefore more desirable to have property-independent *IMs* so that they can be used for any slope condition. A promising option is to use the ordinates of spectral acceleration from short period to long period range to form the vector *IMs*, called "Sa-Vector". The Sa-Vector samples a wide range of frequency content of the ground motions and describes the overall characteristics of the ground motions.

The efficiency of Sa-Vectors is evaluated using three and four spectral ordinates, namely, $Sa(T = 0, 0.2, 1$ s) and $Sa(T = 0, 0.2, 1, 2\ s)$, shown in Figs. 5(d) and (e). Using the Sa-Vectors, high efficiency ($R^2_{adj} = 0.8 - 0.9$) is achieved for $T_s < 1$ s. The efficiency gradually decreases to 0.6 if K_y increases from 0 to 0.4 g. It is interesting to notice that inclusion of the spectral ordinate at 2s, $Sa(T = 2s)$, into the Sa-Vector can significantly improve the efficiency for the range of $1\ s < T_s < 2\ s$. The efficiency of the Sa-Vector can be further improved by using more spectral acceleration ordinates. Figure 5(f) shows R^2_{adj} contours of "$Sa(16T)$," a Sa-Vector consisted of 16 spectral ordinates. The 16 periods are evenly spaced in log between 0.01 and 10 s. Using $Sa(16T)$ results in R^2_{adj} that is greater than 0.85 for all slope conditions.

5 Conclusions

The paper systematically studied the efficiency of various scalar *IMs* and vector *IMs* in predicting seismic slope displacements using a simplified sliding mass model. Although no single *IM* is found to be satisfactorily efficient for all slope conditions, $Sa(1.5T_s)$ and *IA* have been identified as the most efficient scalar *IMs* for flexible and stiff slopes, respectively.

Using vector *IMs* can significant improve the accuracy of seismic displacement prediction and extend the high efficiency to a wider range of slope conditions. Among various vector *IMs* considered, "$Sa(1.5\ T_s) + IA$" can be an effective choice if only two *IMs* should be used. If more *IMs* to be used, the Sa-vector that incorporates at least four spectral ordinates, such as $Sa(T = 0, 0.2, 1, 2$ s), is recommended.

The study provides useful guidance to the development of more efficient empirical prediction models as well as the ground motion selection criteria for time-domain seismic slope analysis. To represent the real seismic hazard at a site, the selected ground motions should capture the variability of the most efficient *IMs*. Among various vector *IMs* considered, the spectral accelerations at multiple spectral periods achieve high efficiency for a wide range of slope conditions. The desirable property of Sa-Vector implies that it is important for the input ground motions to capture the variability of the spectrum accelerations at multiple spectral periods. For this purpose, a ground

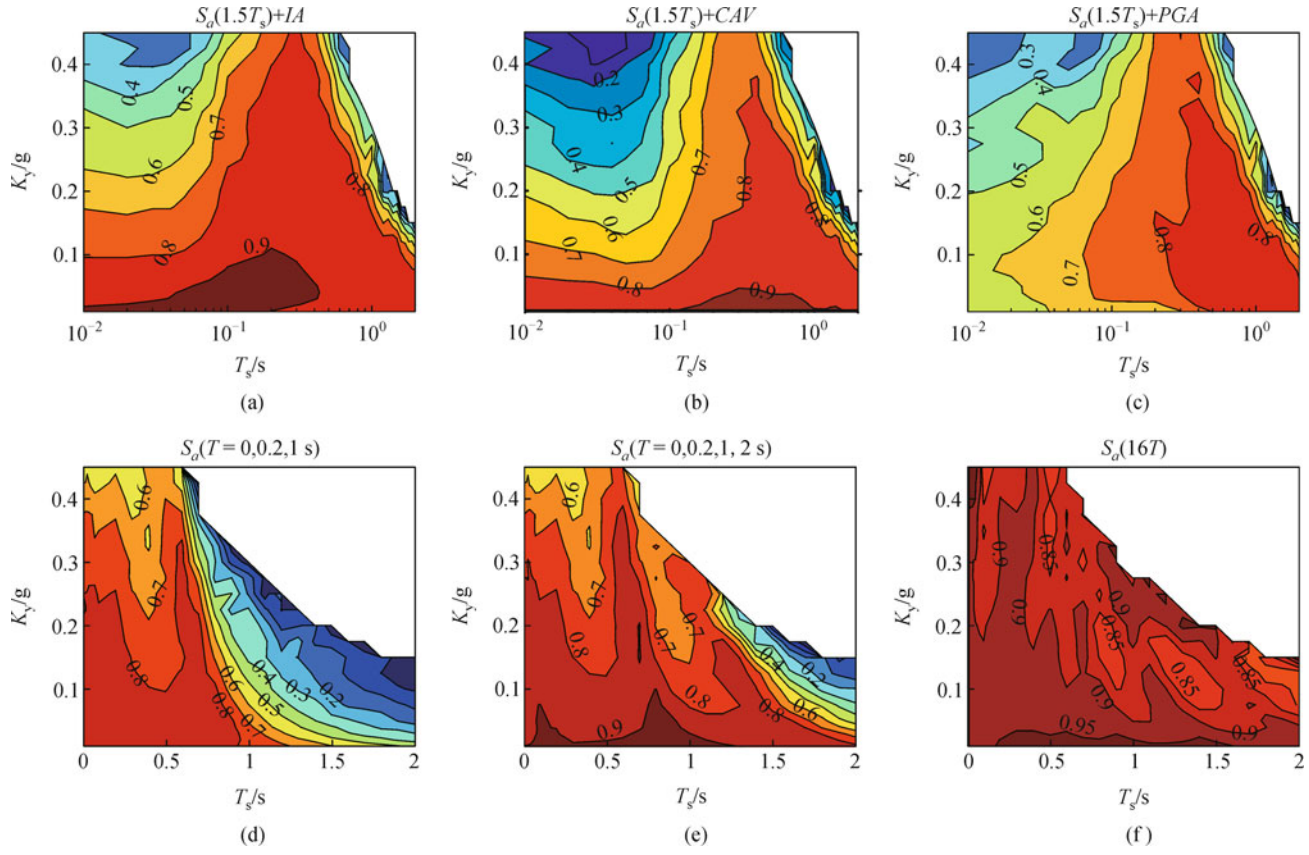

Fig. 5 Contours of adjusted coefficients of determination for vector *IMs*

motion selection method recently proposed [18] can be useful in time-domain seismic slope analysis.

Acknowledgements The research was supported by Hong Kong Research Grants Council (Grants RGC 620311). Support from Li Foundation Heritage Prize is also greatly acknowledged.

References

1. Newmark N M. Effects of earthquakes on dams and embankments. Geotechnique, 1965, 15(2): 139–160
2. Ambraseys N N, Menu J M. Earthquake-induced ground displacements. Earthquake Engineering & Structural Dynamics, 1988, 16 (7): 985–1006
3. Jibson R W. Regression models for estimating coseismic landslide displacement. Engineering Geology, 2007, 91(2–4): 209–218
4. Saygili G, Rathje E M. Empirical prediction models for earthquake-induced sliding displacements of slopes. Journal of Geotechnical and Geoenvironmental Engineering, 2008, 134(6): 790–803
5. Jibson R W. Predicting earthquake-induced landslide displacements using Newmark's sliding block analysis. Transportation Research Record, 1993, 1411: 9–17
6. Romeo R. Seismically induced landslide displacements: a predictive model. Engineering Geology, 2000, 58(3–4): 337–351
7. Watson-Lamprey J, Abrahamson N. Selection of ground motion time series and limits on scaling. Soil Dynamics and Earthquake Engineering, 2006, 26(5): 477–482
8. Rathje E M, Bray J D. Nonlinear coupled seismic sliding analysis of earth structures. Journal of Geotechnical and Geoenvironmental Engineering, 2000, 126(11): 1002–1014
9. Bray J D, Travasarou T. Simplified procedure for estimating earthquake-induced deviatoric slope displacements. Journal of Geotechnical and Geoenvironmental Engineering, 2007, 133(4): 381–392
10. Schnabel P B, Lysmer J, Seed H B. SHAKE—A Computer Program for Earthquake Response Analysis of Horizontally Layered Sites, Earthquake Engineering Research Center, Report No. UCB/EERC-72/12. University of California, Berkeley, 1972
11. Chiou B, Darragh R, Gregor N, Silva W. NGA project strong-motion database. Earthquake Spectra, 2008, 24(1): 23–44
12. Vucetic M, Dobry R. Effect of soil plasticity on cyclic response. Journal of Geotechnical Engineering, 1991, 117(1): 89–107
13. Kramer S L. Geotechnical Earthquake Engineering, Prentice Hall, 1996
14. Arias A. A measure of earthquake intensity. In: Seismic Design for Nuclear Power Plants, Hansen RJ, ed. Cambridge, MA: MIT Press, 1970, 438–483
15. Kempton J J, Stewart J P. Prediction equations for significant duration of earthquake ground motions considering site and near-source effects. Earthquake Spectra, 2006, 22(4): 985–1013
16. Rathje E M, Abrahamson N A, Bray J D. Simplified frequency

content estimate of earthquake ground motions. Journal of Geotechnical and Geoenvironmental Engineering, 1998, 124(2): 150–159

17. Travasarou T, Bray J D. Optimal ground motion intensity measures for assessment of seismic slope displacements. Pacific Conf. on Earthquake Engineering, Christchurch, New Zealand, 2003
18. Wang G. A ground motion selection and modification method capturing response spectrum characteristics and variability of scenario earthquakes. Soil Dynamics and Earthquake Engineering, 2011, 31(4): 611–625

Appendix: The equivalent-linear sliding mass model

The following equivalent-linear, coupled stick-slip model was used to calculate the earthquake-induced permanent displacements.

Assuming that the vibration of the soil mass is dominated by the first mode of vibration, the displacement can be decomposed as

$$u(y,t) = \phi_1(y)Y_1(t), \tag{A1}$$

where $\phi_1(y)$ is the model shape; y is vertical coordinate; $Y_1(t)$ is model displacement. The model shape $\phi_1(y)$ can be analysis as

$$\phi_1(y) = \cos(\pi y/2H), \tag{A2}$$

where H is the height of the sliding mass. It is worth mentioning that incorporating higher mode of vibration is possible, but it will not noticeably affect the solution of the maximum sliding displacement.

If there is no relative movement between sliding mass and the base, the dynamic equation of the sliding mass can be solved as a generalized single-degree-of freedom system

$$\ddot{Y}_1 + 2\lambda\omega_1\dot{Y}_1 + \omega_1^2 Y_1^2 = -L_1/M_1\ddot{u}_g, \tag{A3}$$

where $\ddot{u}_g(t)$ is earthquake acceleration, λ is damping ratio; L_1, M_1 and ω_1 are:

$$\begin{cases} L_1 = \int_0^H m(y)\phi_1(y)\mathrm{d}y; \\ M_1 = \int_0^H m(y)[\phi_1(y)]^2\mathrm{d}y; \\ \omega_1 = 2\pi/T_s, \end{cases} \tag{A4}$$

where $m(y)$ is the mass distribution of sliding block along y-axis, which can be assumed as $m(y) = 1$ for a uniform mass distribution; M_1 is the generalized mass; L_1 is the modal distribution for the earthquake acceleration $\ddot{u}_g(t)$; ω_1 is the rotational frequency, T_s is the initial site period.

Sliding occurs when the driving force exceeds the shear resistance on the interface. The sliding condition is

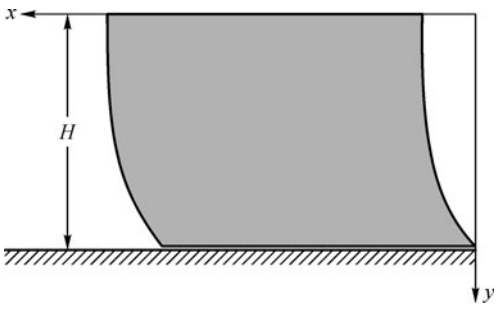

Fig. A1 Sliding mass model

$$-M\ddot{u}_g - L_1\ddot{Y}_1 = \mu Mg, \tag{A5}$$

where M is the total sliding mass, $-M\ddot{u}_g$ is force due to ground acceleration, $L_1\ddot{Y}_1$ is force due to vibration of sliding mass, μ is frictional coefficient of the sliding interface.

When sliding occurs, the equilibrium equation of the system becomes

$$-M(\ddot{u}_g + \ddot{s}) - L_1\ddot{Y}_1 = \mu Mg, \tag{A6}$$

with $\ddot{s}$ being the relative acceleration, which can be solved as

$$\ddot{s} = -\mu g - (L_1/M)\ddot{Y}_1 - \ddot{u}_g. \tag{A7}$$

The above relation can be substituted into the equilibrium equation of the system

$$\ddot{Y}_1 + 2\lambda\omega_1\dot{Y}_1 + \omega_1^2 Y_1^2 = -\frac{L_1}{M_1}(\ddot{u}_g + \ddot{s}), \tag{A8}$$

which reduces to a differential equation with respect to Y_1

$$\ddot{Y}_1 + \frac{2\lambda\omega_1}{d_1}\dot{Y}_1 + \frac{\omega_1^2}{d_1}Y_1^2 = \frac{\mu L_1 g}{d_1 M_1}, \tag{A9}$$

where $d_1 = 1 - L_1^2/(MM_1)$. The above differential equation can be readily solved using numerical methods, so as to obtain the time histories of sliding acceleration, velocity and displacement. When sliding velocity $\dot{s}$ becomes zero, the system is governed by Eq. (A3). Furthermore, only displacement in one direction is permitted such that the permanent displacement is accumulated progressively only in one direction over time.

In the above model, two parameters control the dynamic properties of the slope: the damping ratio λ and the site period T_s. Considering the nonlinearity of the soils, the damping ratio and the site period change according to the earthquake-induced strain levels inside the soils. For vertically propagated shear waves, the site period is related to the shear wave velocity of the soil through

$$T_s = 4H/V_s, \tag{A10}$$

where H is the height of the slope. The shear wave velocity

of the soil is related to the small strain shear modulus via $V_s = \sqrt{G_{max}/\rho_s}$. Earthquake shaking causes the soil modulus to be reduced. Accordingly, the equivalent period T_s^{eqv} is elongated during the shaking, which can be determined using the modulus reduction ratio

$$T_s^{eqv}/T_s = 1/\sqrt{G/G_{max}}. \quad \text{(A11)}$$

To the end, the equivalent linear procedure for computing the permanent seismic displacements of a sliding soil mass is summarized as follows:

1) Specify the initial slope period T_s, the shear wave velocity V_s, the modulus reduction and damping ratio curves for a certain type of soils.

2) Use initial value of T_s and $\lambda = 0$ to solve the dynamics of the system via Eqs. (A1)–(A9).

3) Compute the equivalent shear strain to be 0.65 times maximum shear strain induced inside the sliding mass, i.e., $\gamma^{eqv} = 0.65 \cdot \ddot{Y}_1/H$, where H can be obtained from Eq. (A10).

4) Obtain T_s^{eqv} via Eq. (A11) and λ from the specified modulus reduction and damping curves for that soil type according to the equivalent shear strain.

5) Use updated T_s^{eqv} and λ to solve the dynamics of the system via Eqs. (A1)–(A9).

6) Repeat steps (3) to (5) until the changes in T_s^{eqv} and λ are within tolerances.

7) Finally, obtain the solution of the maximum sliding displacement.

Gang Wang is an assistant professor in the Department of Civil and Environmental Engineering at Hong Kong University of Science and Technology. He is also Director of ASCE Hong Kong Section, and a registered Civil Engineer in California. He received his B.S. and M.S. in Hydraulic Engineering from Tsinghua University, China in 1997 and 2000, respectively, and his Ph.D. in Civil Engineering from University of California, Berkeley, U.S.A. in 2005. He worked as a consulting engineer at Geomatrix Consultants, Oakland, California in 2007–2008. His research interests include geotechnical earthquake engineering, dynamic soil-structure interaction, numerical analysis of geohazards, and micromechanics of heterogeneous materials.